

Resonant nuclear reaction $^{23}\text{Mg} (p, \gamma) ^{24}\text{Al}$ in strongly screening magnetized neutron star crust

Jing-Jing Liu¹, and Dong-Mei, Liu¹

¹ College of Marine Science and Technology, Hainan Tropical Ocean University, Sanya,
Hainan 572022, China

Received _____; accepted _____

Not to appear in Nonlearned J., 45.

¹Corresponding author: syjjliu68@qzu.edu.cn

ABSTRACT

Based on the relativistic theory of superstrong magnetic field (SMF), by using three models of Lai (LD), Fushiki (FGP), and ours (LJ), we investigate the influence of SMFs due to strong electron screening (SES) on the nuclear reaction $^{23}\text{Mg} (p, \gamma) ^{24}\text{Al}$ in magnetars. At relatively low density environment (e.g., $\rho_7 < 0.01$) and $1 < B_{12} < 10^2$, our screening rates are in good agreement with those of LD and FGP. However, in relatively high magnetic fields (e.g., $B_{12} > 10^2$), our reaction rates can be 1.58 times and about three orders of magnitude larger than those of FGP and LD, respectively (B_{12} , ρ_7 are in units of 10^{12}G , 10^7g cm^{-3}). The significant increase of strongly screening rates can imply that more ^{23}Mg will escape from the Ne-Na cycle due to SES in a SMF. As a consequence, the next reaction $^{24}\text{Al} (\beta^+, \nu) ^{24}\text{Mg}$ will produce more ^{24}Mg to participate in the Mg-Al cycle. Thus, it may lead to synthesize a large amount of production of $A > 20$ nuclides in magnetars, respectively.

Subject headings: dense matter— nuclear reactions, nucleosynthesis, abundances— stars: magnetic fields—stars: interiors

1. Introduction

In the dense sites of universe, such as novae, X-ray bursts and supernova, there are explosive hydrogen burning process in high temperature and high hydrogen environments. This burning is called the rapid-proton (rp) process (Wallace et al. 1981). In the stage of hydrogen burning, the proton capture reactions and β^+ -decays (rp-process) will be ignited in the nuclei whose mass numbers $A > 20$. For example, the timescale of the proton capture reaction of ^{23}Mg in the Ne-Na cycle at sufficient high temperature is shorter than that of the β^+ -decay. Therefore, some ^{23}Mg will kindle and escape from the Ne-Na cycle by proton capture. The ^{23}Mg leaks from the Ne-Na cycle into the Mg-Al cycle synthesizing a large amount of heavy nuclei. Thus the reaction $^{23}\text{Mg} (p, \gamma) ^{24}\text{Al}$ in stellar environment is an important reaction for producing heavy nuclei. Wallace et al. (1981) firstly discussed the reaction rate of $^{23}\text{Mg} (p, \gamma) ^{24}\text{Al}$. Then, Iliadis et al. (2001) also investigated this nuclear reaction rate. Kubono et al. (1995) reconsidered the rate by considering four resonances and the structure of ^{24}Al . Based on some new experimental information on ^{24}Al excitation energies, Herndl et al. (1998); Visser et al. (2007), and Lotay et al. (2008) carried out an estimation of the rate. However, they all seem to have overlooked the influence of electron screening on nuclear reaction.

In the pre-supernova stellar evolution and nucleosynthesis, the strong electron screening (SES) is always a challenging and interesting problem. Some works (Bahcall et al. 2002; Liu 2013, 2014, 2016; Liu et al. 2017,?) have been done on stellar weak-interaction rates and thermonuclear reaction rates. In the high-density surrounding, some SES models have been widely investigated, such as Salpeter model (Salpeter 1954; Salpeter et al. 1969), Graboske model (Graboske et al. 1973), and Dewitt model (Dewitt et al. 1976). Recently these issues were discussed by Liolios et al. (2000, 2001), Kravchuk et al. (2014), and Liu (2013). However, they neglected the effects of SES on thermonuclear reaction rate in

superstrong magnetic field (SMF).

It is widely known that nuclear reaction rates at low energies play a key role in energy generation in stars and the stellar nucleosynthesis. The bare reaction rates are modified in stars by the screening effects of free and bound electrons. The knowledge of the bare nuclear reaction rates at low energies is important not only for the understanding of various astrophysical nuclear problems, but also for assessing the effects of host material in low energy nuclear fusion reactions in matter.

It is universally accepted that the surface dipole magnetic field strengths of magnetars are in a range from 10^{13} to 10^{15} G (Peng et al. 2007; Gao et al. 2011, 2013, 2015, 2017,?; Li et al. 2016; Lai 2001). The momentum space of the electron gas is modified substantially by so intense magnetic fields. The electron Fermi energy and nuclear reaction are also affected greatly by a SMF in magnetars.

Anomalous x-ray pulsars (AXPs) and soft gamma-ray repeaters (SGRs) are conceived as magnetars, which are a kind of special pulsars powered by their magnetic energy (Duncan 1992). The Fermi energy of the electrons will increase with magnetic field and quantum effects of electron gas will be very obvious in a SMF. As we all know, the positive energy levels of electrons must abide by Landau quantization. The distribution of the electron in the momentum space will be strongly modified by a SMF. Some authors discussed this issue in detail in strong magnetic fields of magnetars. For instance, Gao et al. (2015, 2017,?) investigated not only the spin-down and magnetic field evolutions, but also the electron Landau level effects on emission properties of magnetars.

In this paper, according to the relativistic theory in a SMF (Peng et al. 2007; Gao et al. 2011, 2013, 2015, 2017), we discuss the problem of SES and then investigate the effect of SES on the thermonuclear reaction within three different models (i.e., our model (LJ), Lai model (LD)(Lai et al. 1991; Lai 2001), and Fushiki model (FGP)(Fushiki et al. 1989)) on

the surface of magnetars.

Our work differs from previous work of Liu (2016) about the discussion of nuclear reaction rates. Firstly, in Liu (2016), though we cited several work from Gao et al., but it is not familiar to the calculations involved in electron Fermi energy in a superhigh magnetic field, a non-relativistic electron cyclotron solution was applied when calculating the rates. Secondly, our previous work Liu (2016) did not give a comparison among LJ, LD, and FGP models in the case with a SMF. Finally, we analyze the nuclear reaction rates in a SMF and also give a comparison for our model with Dewitt model(Dewitt et al. 1976), and Liolios model(Liolios et al. 2000), in which the SMF were not taken into consideration. Maybe SES universally occur in pulsars, and the screening rate calculations in a SMF is of importance to the future studies on cooling, nucleosynthesis, and emission properties of magnetars.

In this paper, following the works of Peng et al. (2007), and Gao et al. (2011, 2013, 2015, 2017), we calculate the resonant reaction rates in the case with SMF and without SMF in several screening models. In the case of the former, the results from LD and FGP models will be compared with those of our model, while in the latter case, the results from Dewitti and Liolio models also will be compared. We derive new results for SES theory and the screening rates for nuclear reaction in relativistic strong magnetic fields.

The article is organized as follows. In the next Section, we analyse three SES models in a SMF of magnetars. In Section 3 we discuss the effects of SES on the proton capture reaction rate of ^{23}Mg , in which the four resonances contributions will also be considered. The results and discussions will be shown in Section 4. The article is closed with some conclusions in Section 5.

2. The SES in SMF

In astrophysical systems, the SMF may have significant influence on the quantum processes. In this Section, we will study three models of the electron screening potential (ESP) in SMF, i.e., LJ model, LD model, and FGP model.

2.1. ESP in our model

The rate of nuclear reaction in high density matter is affected by the fact that the clouds of the electrons surrounding nuclei alter the interactions among nuclei. The positive energy levels of electrons in SMF are given by (Landau et al. 1977)

$$\frac{\varepsilon_n}{m_e c^2} = \left[\left(\frac{p_z}{m_e c} \right)^2 + 1 + 2 \left(n + \frac{1}{2} + \sigma \right) b \right]^{1/2} = (p_z^2 + \Theta)^{1/2}, \quad (1)$$

where $\Theta = 1 + 2 \left(n + \frac{1}{2} + \sigma \right) b$, $n = 0, 1, 2, 3, \dots$, $b = \frac{B}{B_{\text{cr}}} = 0.02266 B_{12}$, B_{12} is the magnetic fields in units of 10^{12}G , i.e., $B_{12} \equiv B/10^{12}\text{G}$, $B_{\text{cr}} = \frac{m_e^2 c^3}{e \hbar} = 4.414 \times 10^3 \text{G}$ is the electron quantum critical magnetic field, and p_z is the electron momentum along the field, σ is the spin quantum number of an electron, when $n = 0, \sigma = 1/2$, and when $n \geq 1, \sigma = \pm 1/2$.

In an extremely strong magnetic field ($B \gg B_{\text{cr}}$), the Landau column becomes a very long and narrow cylinder along the magnetic field. According to the Pauli exclusion principle, the electron number density should be equal to its microscopic state density. By introducing the electron Landau level stability coefficient, the Fermi energy of the electron is given by (Gao et al. 2013; zhu et al. 2018)

$$\begin{aligned} U_{\text{F}} &= 5.91 \times 10^4 \left(\frac{B}{B_{\text{cr}}} \right)^{1/6} \left(\frac{\rho Y_e}{\rho_0 \times 0.00564} \right)^{1/3} \\ &= 5.91 \times 10^4 \left(\frac{B}{B_{\text{cr}}} \right)^{1/6} \left(\frac{n_e}{0.00564 \times \rho_0 N_{\text{A}}} \right)^{1/3} \text{keV}, \end{aligned} \quad (2)$$

where $\rho_0 = 2.8 \times 10^{14} \text{g/cm}^3$ is the standard nuclear density.

In order to evaluate the Thomas-Fermi screening wave-number $K_{\text{TF}}^{\text{LJ}}$, we defined a parameter $D^{\text{LJ}}(U_e)$ and according to Eq.(3), we have

$$n_e = 0.00564\rho_0 N_A \left(\frac{U_F}{5.91 \times 10^4 b^{1/6}} \right)^3 \quad (3)$$

$$\begin{aligned} D^{\text{LJ}}(U_F) &= \frac{\partial n_e}{\partial U_F} = \frac{\partial}{\partial U_F} \left(0.00564\rho_0 N_A \left(\frac{U_F}{5.910 \times 10^4 b^{1/6}} \right)^3 \right) \\ &= 4.9913 \times 10^7 n_e^{2/3} b^{-1/6} \quad \text{cm}^{-3} \text{ KeV}^{-1}. \end{aligned} \quad (4)$$

According to Eq.(5), the Thomas-Fermi screening wave-number $K_{\text{TF}}^{\text{LJ}}$ is given by (Ashcroft et al. 1976)

$$\begin{aligned} (K_{\text{TF}}^{\text{LJ}})^2 &= 4\pi e^2 D^{\text{LJ}}(U_F) = 4\pi e^2 \frac{\partial n_e}{\partial U_F} \\ &= 6.269 \times 10^7 e^2 (n_e)^{2/3} b^{-1/6} \quad \text{cm}^{-3}. \end{aligned} \quad (5)$$

By using the uniform electron gas model (Kadomtsev 1971), the binding energy of the magnetized condensed matter at zero pressure can be estimated. The energy per cell can be written as

$$E_{\text{total}} = E_{\text{k}} + E_{\text{latt}} = \frac{3\pi^2 e^2 z_j^3}{8b_1^2 r_i^6} + \frac{9e^2 z_j^{5/3}}{10r_e} \quad \text{MeV}, \quad (6)$$

where the first term is the kinetic energy and the second term is the lattice energy.

$r_i = z^{1/3} r_e a_0$ is the Wigner-Seitz cell radius, $a_0 = 0.529 \times 10^{-8} \text{cm}$ is the Bohr radius, and

$r_e = (3/4\pi n_e)^{1/3}$ is the mean electron spacing. z_j is the charge number of the species j .

$b_1 = B/B_0 = 425.4B_{12} = 1.9773 \times 10^4 b$ and $B_0 = m_e^2 c e^3 / \hbar^3 = 2.3505 \times 10^{-9} \text{G}$ is the natural (atomic) unit for the field strength (Lai 2001). For the zero-pressure condensed matter, we

require $dE_{\text{total}}/dr_i = 0$, so we have

$$r_i = r_{i0} = 0.0371 z_j^{1/5} b^{-2/5} a_0 \quad \text{cm}. \quad (7)$$

By using linear response theory, the energy correction per cell due to non-uniformity is

given by (Lattimer et al. 1985)

$$\begin{aligned} E_{\text{TF}}^{\text{LJ}}(r_i, z_j) &= -\frac{18}{175} (K_{\text{TF}}^{\text{LJ}} r_i)^2 \frac{(z_j e)^2}{r_i} \\ &= -\frac{1.30 \times 10^{-6} e^6 (n_e)^{4/3} z_j^{9/5}}{b^{11/15}} \text{ MeV}. \end{aligned} \quad (8)$$

For the relativistic electrons, the influence from exchange free energy were discussed by Refs. Stolzmann et al. (1996); Yakovlev et al. (1989). Their works showed that the correlation correction is very small. Therefore, in this paper we have neglected the correction of Coulomb exchange free energy interaction in the electron gas model. By taking into consideration of the Coulomb energy and Thomas-Fermi correction due to non-uniformity of the electron gas, the energy per cell should be corrected as

$$E_s^{\text{LJ}}(r_i, z_j) = E_k(r_i, z_j) - U_{\text{coul}}(r_i, z_j) - E_{\text{TF}}^{\text{LJ}}(r_i, z_j). \quad (9)$$

For two interaction nuclides, the energy required to bring two nuclei with nuclear charge numbers z_1 and z_2 so close together that they essentially coincide differs from the bare Coulomb energy by an amount which in the Wigner-Seitz approximation is

$$U_{\text{sc}} = E_s(r_i, z_{12}) - E_s(r_i, z_1) - E_s(r_i, z_2), \quad (10)$$

where $z_{12} = z_1 + z_2$. If the electron distribution is rigid, the contribution to from E_s the bulk electron energy cancel in expression (11), and the screening potential is simply given as

$$\begin{aligned} U_{\text{sc}} &= E_{\text{coul}}(r_i, z_{12}) - E_{\text{coul}}(r_i, z_1) - E_{\text{coul}}(r_i, z_2) \\ &= 6.5984 \times 10^4 b^{2/5} (z_{12}^{9/5} - z_1^{9/5} - z_2^{9/5}) \text{ MeV}, \end{aligned} \quad (11)$$

where we assume the electron density is uniform, and the screening potential is independent of the magnetic field.

From expression (9), the change of the screening potential due to the compressibility of the electrons in the zero-pressure magnetized condensed matter can be obtained as

$$\begin{aligned}\delta E_{\text{TF}}^{\text{LJ}} &= -\frac{18}{175}(K_{\text{TF}}^{\text{LJ}}r_i)^2 \frac{e^2(z_{12}^2 - z_1^2 - z_2^2)}{r_i} \\ &= -\frac{1.30 \times 10^{-6} e^6 n_e^{4/3} (z_{12}^{9/5} - z_1^{9/5} - z_2^{9/5})}{b^{11/15}}.\end{aligned}\quad (12)$$

In accordance with the above discussions, the total screening potential is the sum of the screening potential with a uniformity distribution and a corrected screening potential with a non-uniformity distribution. The screening potential in SMF is given by

$$U_{\text{sc}}^{\text{LJ}} = U_{\text{sc}} + \delta E_{\text{TF}}^{\text{LJ}}. \quad (13)$$

2.2. ESP in LD model

Lai (2001) and Lai et al. (1991) discussed the equation of state and the electron energy in a SMF. In a SMF the electron number density n_e is related to the chemical potential U_e by

$$\begin{aligned}n_e &= \frac{1}{(2\pi\hat{\rho})^2\hbar} \sum_0^\infty g_{n0} \int_{-\infty}^{+\infty} f dp_z \\ &= \frac{1}{(2\pi\hat{\rho})^2\hbar} \sum_0^\infty g_{n0} \int_{-\infty}^{+\infty} [1 + \exp(\frac{E - U_e}{kT})]^{-1} dp_z,\end{aligned}\quad (14)$$

where $\hat{\rho} = (\hbar c/eB)^{1/2} = 2.5656 \times 10^{-10} B_{12}^{1/2} \text{cm}$ is the electron cyclotron radius (the characteristic size of the wave packet), and $E = [c^2 p_z^2 + m_e c^4 (1 + nb)]^{1/2}$ is the free electron energy, g_n is the spin degeneracy of the Landau level, $g_{00} = 1$ and $g_{n0} = 2$ for $n \geq 1$, and the Fermi-Dirac distribution is given by

$$f = [1 + \exp(\frac{E - U_e}{kT})]^{-1}. \quad (15)$$

The electron Fermi energy including the electron rest mass is given by

$$n_e = \frac{1}{2\pi^{3/2}\lambda_{Te}\tilde{\rho}^2} \sum_{(n=0)}^{\infty} g_n I_{-1/2}\left(\frac{U_e - n\hbar\omega_{ce}}{kT}\right), \quad (16)$$

where the thermal wavelength of the electron is $\lambda_{Te} = (2\pi\hbar^2/m_e kT)^{1/2}$, and the Fermi integral is written as

$$I_n(y) = \int_0^{\infty} \frac{x^n}{\exp(x-y) + 1} dx. \quad (17)$$

The binding energy of the magnetized condensed matter at zero pressure can be estimated using the uniform electron gas model. Under the condition of super-strong magnetic field, the Fermi energy U_F is less than the cyclotron energy $\hbar\omega_{ce}$, the electrons only occupy the ground Landau level. According to their viewpoint of (Lai 2001), the Thomas-Fermi screening wave-number is given by

$$(K_{TF}^{LD})^2 = 4\pi e^2 D^{LD}(\varepsilon_F) = 4\pi e^2 \frac{\partial n_e}{\partial \varepsilon_F} = 4\pi e^2 \frac{\partial n_e}{\partial U_F}, \quad (18)$$

where $\partial n_e/\partial \varepsilon_F$ is the density of states per unit volume at the Fermi surface. $\varepsilon_F = P_F^2/2m_e$. From Eq.(6.16) of Lai (2001), so we have

$$D^{LD} = \frac{\partial n_e}{\partial \varepsilon_F} = \frac{3.79 \times 10^6 b^2 r_e^3}{e^2}. \quad (19)$$

The Thomas-Fermi screening wave-number will be given by

$$K_{TF}^{LD} = \left(\frac{4}{3\pi^2}\right)^{1/2} b_1 r_e^{3/2} = 6.901 \times 10^3 b r_e^{3/2}. \quad (20)$$

Using the linear response theory, the energy correction (in atomic units) per cell due to non-uniformity can be calculated and gives by (Lai 2001)

$$E_{TF}^{LD}(r_i, z_j) = -\frac{18}{175} (K_{TF}^{LD} r_i)^2 \frac{e^2 z_j^2}{r_i} = -0.0139 b_1^2 r_i^4 z_j. \quad (21)$$

The uniform electron gas model can be improved by taking into consideration of the Coulomb energy and Thomas-Fermi correction due to non-uniformity of the electron gas.

When the electron density is assumed to be uniform, the screening potential is independent of the magnetic field. The change of the screening potential due to the compressibility of the electrons for the zero-pressure magnetized condensed matter can be obtained

$$\delta E_{\text{TF}}^{\text{LD}} = -2.5236 \times 10^{-4} b^{2/5} (z_{12}^{9/5} - z_1^{9/5} - z_2^{9/5}). \quad (22)$$

When we summed of a screening potential with a uniformity distribution and a corrected screening potential with a non-uniformity distribution, the screening potential in a SMF is given by

$$U_s^{\text{LD}} = U_{\text{sc}} + \delta E_{\text{TF}}^{\text{LD}}. \quad (23)$$

2.3. ESP in FGP model

The influence of SES in a SMF on nuclear reaction was also discussed in detail by Fushiki et al. (1989) (hereafter FGP). The electron Coulomb energy by an amount which in the Wigner-Seitz approximation in a SMF was given by

$$U_{\text{sc}}^{\text{FGP}} = E_{\text{atm}}(r_i, z_{12}) - E_{\text{atm}}(r_i, z_1) - E_{\text{atm}}(r_i, z_2), \quad (24)$$

where $E_{\text{atm}}(r_i, z_j)$ is the total energy of Wigner-Seitz cell. If the electron distribution is rigid, the contribution to $E_{\text{atm}}(r_i, z_j)$ from the bulk electron energy cancel, the electron screening potential at high density can be expressed as

$$U_{\text{sc}}^{\text{FGP}} = E_{\text{latt}}(r_i, z_{12}) - E_{\text{latt}}(r_i, z_1) - E_{\text{latt}}(r_i, z_2), \quad (25)$$

where $E_{\text{latt}}(r_i, z_j)$ is the electrostatic energy of Wigner-Seitz cell and $E_{\text{atm}}(r_i, z_j) = -0.9z_j^{5/3}e^2/r_e$. Due to the influence of the compressibility of the electron, the change in the screening potential is given by (Fushiki et al. 1989)

$$\begin{aligned} \delta U_s^{\text{FGP}} &= -\frac{54}{175} \left(\frac{e^2}{r_e}\right) \frac{1}{n_e} \frac{\partial n_e}{\partial U_e} [(z_{12})^{7/3} - (z_1)^{7/3} - (z_2)^{7/3}] \\ &= -\frac{54}{175} \left(\frac{e^2}{r_e}\right) \frac{1}{n_e} D^{\text{FGP}} [(z_{12})^{7/3} - (z_1)^{7/3} - (z_2)^{7/3}], \end{aligned} \quad (26)$$

where

$$D^{\text{FGP}} = 823.1481 \frac{r_e n_e}{e^2} \left(\frac{\overline{A}}{z}\right)^{4/3} \rho^{-4/3} B_{12}^2. \quad (27)$$

The Thomas-Fermi screening wave-number will be given by

$$(K_{\text{TF}}^{\text{FGP}})^2 = 1.0344 \times 10^4 r_e n_e \left(\frac{\overline{A}}{z}\right)^{4/3} \rho^{-4/3} B_{12}^2. \quad (28)$$

Thus, the corresponding result for the changes in the screening potential in a SMF is

$$\begin{aligned} \delta U_s^{\text{FGP}} &= -0.254 \left(\frac{\overline{A}}{z}\right)^{4/3} \rho^{-4/3} B_{12}^2 [(z_{12})^{7/3} - (z_1)^{7/3} - (z_2)^{7/3}] \\ &= -494.668 \left(\frac{\overline{A}}{z}\right)^{4/3} \rho^{-4/3} b^2 [(z_{12})^{7/3} - (z_1)^{7/3} - (z_2)^{7/3}] \text{MeV}, \end{aligned} \quad (29)$$

where $(\overline{A/z})$ is the average ratio of A/z , which corresponding to the mean molecular weight per electron. Thus the electron screening potential in a SMF of FGP model is given by

$$U_s^{\text{FGP}} = U_{\text{sc}} + \delta E_{\text{TF}}^{\text{FGP}} = U_{\text{sc}} + \delta U_s^{\text{FGP}}. \quad (30)$$

3. Resonant reaction process and rates

3.1. Calculations of resonant reaction rates with and without SES

The reaction rates are summed of contribution from the resonant reaction and non-resonant reaction. In the case of a narrow resonance, the resonant cross section σ_r is approximated by a Breit-Wigner expression (Fowler et al. 1967)

$$\sigma_r(E) = \frac{\pi\omega}{\kappa^2} \frac{\Lambda_i(E)\Lambda_f(E)}{(E - E_r^2) + \frac{\Lambda_{\text{total}}^2(E)}{4}}, \quad (31)$$

where κ is the wave number, the entrance and exit channel partial widths are $\Lambda_i(E)$ and $\Lambda_f(E)$, respectively. $\Lambda_{\text{total}}(E)$ is the total width, and the statistical factor, ω is given by

$$\omega = (1 + \delta_{12}) \frac{2J + 1}{(2J_1 + 1)(2J_2 + 1)}, \quad (32)$$

where the spins of the interacting nuclei and the resonance are J_1 , and J_2 , respectively, δ_{12} is the Kronecker symbol.

The partial widths is dependent on the energy, and can be written as(Lane et al. 1958)

$$\Lambda_{i,f} = 2\vartheta_{i,f}^2 \psi_l(E, a) = \Lambda_{i,f} \frac{\psi_l(E, a)}{\psi_l(E_f, a)}. \quad (33)$$

The penetration factor ψ_l is associated with l and a , which are the relative angular momentum and the channel radius, respectively. $a = 1.4(A_1^{1/3} + A_2^{1/3})$ fm. $\Lambda_{i,f}$ is the partial energy widths at the resonance process. E_r and $\vartheta_{i,f}^2$ is the reduced widths, given by

$$\vartheta_{i,f}^2 = 0.01\vartheta_w^2 = \frac{0.03\hbar^2}{2Aa^2}. \quad (34)$$

Based on the above analysis, in the phases of explosive stellar burning, the narrow resonance reaction rates without SES are determined by (Schatz et al. 1998; Herndl et al. 1998)

$$\begin{aligned} \lambda_r^0 &= N_A \langle \sigma v \rangle_r = 1.54 \times 10^{11} (AT_9)^{-3/2} \\ &\times \sum_i \omega \gamma_i \exp(-11.605 E_{r_i}/T_9) \quad \text{cm}^3 \text{mol}^{-1} \text{s}^{-1}, \end{aligned} \quad (35)$$

where N_A is Avogadro's constant, A is the reduced mass of the two collision partners, E_{r_i} is the resonance energies and T_9 is the temperature in unit of 10^9 K. The $\omega \gamma_i$ is the strength of resonance in units of MeV and given by

$$\omega \gamma_i = (1 + \delta_{12}) \frac{2J + 1}{(2J_1 + 1)(2J_2 + 1)} \frac{\Lambda_i \Lambda_f}{\Lambda_{\text{total}}}. \quad (36)$$

On the other hand, due to SES the reaction rates of narrow resonance is given by

$$\begin{aligned} \lambda_r^s &= F_r N_A \langle \sigma v \rangle_r \\ &= 1.54 \times 10^{11} (AT_9)^{-3/2} \sum_i \omega \gamma_i \exp(-11.605 E'_{r_i}/T_9) \\ &= 1.54 \times 10^{11} F_r (AT_9)^{-3/2} \\ &\times \sum_i \omega \gamma_i \exp(-11.605 E_{r_i}/T_9) \quad \text{cm}^3 \text{mol}^{-1} \text{s}^{-1}, \end{aligned} \quad (37)$$

where F_r is the screening enhancement factor (hereafter SEF). The values of E'_{r_i} should be measured by experiment, but it is too hard to provide sufficient data. In general and approximate analysis, we have $E'_{r_i} = E_{r_i} - U_0 = E_{r_i} - U_s$.

3.2. The screening model of resonant reaction rates in the case without SMF

3.2.1. Dewitt model

Dewitt et al. (1976) discussed the problem of thermonuclear ion-electron screening at some densities. Based on a statistical mechanical theory for the screening function, the influence of the electron screening on the nuclear reaction process also was investigated in their paper. The strong electron screening potential function is given by (Dewitt et al. 1976)

$$\begin{aligned}
 H_{12}^{\text{sc}} = & \frac{e^2}{r_e kT} \{0.9(\bar{z})^{1/3}(z_{12}^{5/3} - z_1^{5/3} - z_2^{5/3}) \\
 & + c_1(\bar{z})^{2/3}(z_{12}^{4/3} - z_1^{4/3} - z_2^{4/3})\} \\
 & + [c_2(\bar{z})^{-2/3}(z_{12}^{2/3} - z_1^{2/3} - z_2^{2/3})],
 \end{aligned} \tag{38}$$

where $c_1 = 0.2843$ and $c_2 = 0.4600$, and the \bar{z} , the average charge of ionic, is given by

$$\bar{z} = \sum_i z_i f_i = \sum_i z_i \frac{n_i}{n_I}, \tag{39}$$

where n_i and n_I are the ion densities of nuclear species i and I of the total system, respectively.

The screening enhancement factor (hereafter SEF) in Dewitt model is written as

$$F_r^0(\text{Dew}) = \exp(H_{12}^{\text{sc}}). \tag{40}$$

3.2.2. Liolios model

At astrophysical energies the electron-screening acceleration in laboratory fusion reactions always play a key role and is an interesting problem for astrophysics. Based on a mean-field model, Liolios et al. (2000) studied the screened nuclear reactions at astrophysical energies. The electron screening potential in Liolios screened Coulomb model is given as (Liolios et al. 2000)

$$U_0^{\text{Lios}} = \frac{15}{8} \frac{z_1 z_2 e^2}{\Xi}, \quad (41)$$

where

$$\Xi = \left(\frac{15}{8\pi z_i^2}\right)^{1/3} a_0 = 0.8853 a_0 (z_1^{2/3} + z_2^{2/3})^{1/2}, \quad (42)$$

The SEF for the resonant reaction in Liolios model is

$$F_r^0(\text{Lios}) = \exp\left(\frac{11.605 U_0^{\text{Lios}}}{T_9}\right). \quad (43)$$

3.3. The screening model of resonant reaction rates in SMFs

In this Subsection, we will discuss the screening potential in the strong screening limit. The dimensionless parameter (Γ), which determines whether or not correlations between two species of nuclei (z_1, z_2) are important, is given by

$$\Gamma = \frac{z_1 z_2 e^2}{(z_1^{1/3} + z_2^{1/3}) r_e k T}, \quad (44)$$

Under the conditions of $\Gamma \gg 1$, the nuclear reaction rates will be influenced appreciably by SES. According to the above three SES models (LD, FGP, LJ) in SMFs, the three enhancement factors for resonant reaction process in SMFs can be expressed as follows

$$F_r^{\text{B}}(\text{LD}) = \exp\left(\frac{11.605 U_s^{\text{LD}}}{T_9}\right), \quad (45)$$

$$F_r^{\text{B}}(\text{FGP}) = \exp\left(\frac{11.605 U_s^{\text{FGP}}}{T_9}\right), \quad (46)$$

$$F_r^B(\text{LJ}) = \exp\left(\frac{11.605U_s^{\text{LJ}}}{T_9}\right). \quad (47)$$

4. Numerical results

4.1. Analysis of the results on a SEF

The strong magnetic fields modify significantly the properties of the matter and always play a critical role in astronomical conditions. Figure 1 presents the variations of ESP as a function of B_{12} for our SES model. The SMF has only a slight influence on ESP when $B_{12} > 3 \times 10^3$ and $\rho_7 < 1$. But the ESP increases greatly when $B_{12} < 1.4 \times 10^3$ and $\rho_7 < 1$ (B_{12} , ρ_7 are in units of 10^{12}G , 10^7g cm^{-3} , respectively). Numerical results in our model show that the maximum value of ESP reaches to 0.1 MeV. Figure 2 (a) presents the ESP in LD model as a function of B_{12} . The ESP increases rapidly and reaches the maximum value of 0.008442 MeV at $B_{12} = 80$, then decreases with increasing of a SMF.

Based on the Thomas-Fermi and Thomas-Fermi-Dirac approximations, Fushiki et al. (1989) analyzed the electron Fermi energy, electron Landau level, and SES problem in a SMF. The results show that, as a consequence of the field dependence of the screening potential, magnetic fields can significantly increase nuclear reaction rates (Fushiki et al. 1989). According to electron screening model of Ref.(Fushiki et al. 1989) (hereafter FGP model) in a SMF, Figure 2 (b) shows the ESP as a function of B_{12} under some typical astrophysical conditions. The ESP increases greatly when $B_{12} < 10^3$ and gets to the maximum value of 0.0188 MeV at $B_{12} = 580.7$ and $\rho_7 = 0.1$. Then the ESP decreases around two orders of magnitude when $10^3 < B_{12} < 2 \times 10^3$ at $\rho_7 = 0.1$.

The influence of SES in a SMFs on nuclear reaction is mainly reflected by the SEF. We discuss the influence of SES on SEF by three models (LD, FGP, LJ) from Figure 3 to Figure 4. One finds that the SEF of LD model is a sensitive parameter for a SMF and

temperature. The maximum value of a SEF is about 1.632 for $B_{12} = 78.17$ and $T_9 = 0.2$, as shown in Figure 3, where T_9 is the temperature in units of 10^9K . But for $B_{12} > 219.3$ the SEF is less than 1.001. Figure 4 presents the SEF as function of B_{12} of FGP and LJ models. From sub-figures 4(a) and 4 (b), one find that the shifty trend of SEF in FGP model is in good agreement with those of LD at low density (e.g. $\rho_7 = 0.01$). The maximum value of SEF of FGP model is about 1.66 for $B_{12} = 84.18$ and $\rho_7 = 0.01$. On the contrary, the SEF increases with increasing of B_{12} at relatively high density (e.g. $\rho_7 = 1$), then gets to the maximum value of 5.166 at $T_9 = 0.2$. Sub-figures 4(c) and 4(d) show that in LJ model show that the SEF increases with increasing of B_{12} , and the maximum value will reach up to 5.056 for $B_{12} = 1000$, $T_9 = 0.2$ and $\rho_7 = 0.01$.

In Figure 5, some comparisons of the resonant SEF are shown among the models of LJ, LD, and FGP for typical astronomical conditions in a SMF. The results of LD model are well agreement with those of FGP for relatively low density (e.g., $\rho_7 \leq 0.01$). Nevertheless, the SEF of our model decreases placidly with the increasing of B_{12} and T_9 to compare with those of LD and FGP.

The SES problem always plays important roles in stellar evolution process. Based on a statistical mechanical theory for the screening function, Dewitt et al. (1976) investigated the influence of the electron screening on nuclear reaction. Based on a mean-field model, Liolios et al. (2000) also studied the effect about screened nuclear reactions. However, they neglected the influence of SMFs on SES. We compare the SEF of the two models (Dewitt, and Liolios model) with those of LD, FGP, and LJ. One can conclude that the SEF of Dewitt model is larger than those of other three SES models for $B_{12} < 140$, $\rho_7 = 0.01$ and $T_9 < 0.17$, shown as in Figure 6. However, when $T_9 < 0.18$, $\rho_7 = 0.01$, the results of our model are larger than those of Dewitt and Liolios. At a relatively high density (e.g., $\rho_7 = 0.1$), the SEFs of LD, FGP and LJ models decrease due to SMFs and is lower

than those of Dewitt model. The results obtained by Dewitt et al. (1976) amount to an overestimation of the screening effect because of their neglect of spatial dependence of the screening function.

Table 1 shows some information of SEF for the five typical models at some astronomical conditions. The results of LD, FGP, and LJ are always lower than those of Liolios and Dewitt due to a SMF. The SEF of our model decreases very greatly with increasing of density and temperature when $B_{12} = 10^3$. It is because that the ESP increases very rapidly as SMF increases. The higher the ESP, the larger the influence on SES becomes. On the contrary, the SEF of LD decreases with increasing of magnetic fields because ESP is reduced. The SEF of FGP model gets to the maximum of 1.929 when $B_{12} = 10^3$, $\rho_7 = 1$, $T_9 = 0.5$ and then decreases slowly as the density and temperature increase.

The Thomas-Fermi screening wave-number K_{TF} is a very key parameter, which strongly depends on the electron number density and ESP. In consequence the electron number density and ESP will play important roles in a SMF. Lai et al. (1991), analyzed in detail the electron Fermi energy and electron number density in a SMF based on the works of Canuto et al. (1968, 1971); Kubo. (1965), and Pathria (2003). By using the uniform electron gas model and linear response theory, Lai (2001) discussed the electron energy (per cell) corrections due to non-uniformity in a SMF. According to their theory, we study the ESP and the SES model (i.e., LD model). The results show that the ESP decreases as the magnetic fields increase due to the diminution of electron chemical potential. The LD model is valid only in the condition of $K_{TF}r_i \ll 1$ at lower densities, because they investigated the non-uniformity effect only through detailed electronic (band) structure calculations.

The electron chemical potential is a pivotal parameter, which is closely related to the electron number density and exchange energy. Based on Thomas-Fermi-Dirac

approximation, it is given as (Fushiki et al. 1989)

$$U_F = U_e = \frac{\partial w_{\text{ex}}}{\partial n_e} = \frac{r_{\text{cyc}}}{\pi a_0} \hbar \omega_0 n I(n), \quad (48)$$

where w_{ex} is the exchange energy and $I(n)$ can be found in Ref. (Fushiki et al. 1989). By using the linear response theory, Fushiki et al. (1989) discussed the exchange energy and electron chemical potential in the lowest Landau level for non-uniformity electron gas in a SMF. They analyzed the SES problem in a SMF and their results shown that a SMF only the lowest Landau level is occupied by electrons on the condition of $r_e > (3\pi/8)^{1/3} r_{\text{cyc}}$ or equivalently $\rho < 7.04 \times 10^3 B_{12}^{3/2} (\text{A/z}) \text{g/cm}^3$. The cyclotron radius in the lowest Landau level orbital is give by $r_{\text{cyc}} = (2\hbar c/eB)^{1/2} \simeq 3.36 \times 10^{-10} B_{12}^{-1/2}$. FGP used the expression of $n_e \partial n_e / \partial U_F = (3/2) n_e / U_F$ in dealing with $\partial n_e / \partial U_F$. In FGP model, they thought at high density the exchange correction is very small, thus they neglected the exchange correction to $\partial n_e / \partial U_F$ and had $n_e \partial n_e / \partial U_F = (1/2) n_e / U_F$ in a SMF. Due to different ways of dealing with exchange correction under this condition, the SEF of FGP model has some difference compared with other SES models.

According to statistical physics the microscopic state number $dx dy dz dp_x dp_y dp_z$ can be given by $dx dy dz dp_x dp_y dp_z / h^3$ in a 6-dimension phase-space. The number of states occupied by completely degenerate relativistic electrons per volume is calculated by (Canuto et al. 1968, 1971)

$$\begin{aligned} N_{\text{phase}} &= \sum_{p_x} \sum_{p_y} \sum_{p_z} = \frac{1}{h^3} \int_{-\infty}^{\infty} \int_{-\infty}^{\infty} \int_{-\infty}^{\infty} dp_x dp_y dp_z \\ &= \frac{1}{h^3} \int_0^{p_F} dp_z \int_0^{\infty} p_{\perp} dp_{\perp} \int_0^{2\pi} d\theta = \frac{\pi p_F}{h^3} \int_0^{\infty} dp_{\perp}^2, \end{aligned} \quad (49)$$

where $\theta = \tan^{-1} p_y / p_x$, $p_{\perp}^2 \rightarrow m^2 c^4 \frac{B}{B_{\text{cr}}} 2n$, So, $\int_0^{\infty} dp_{\perp}^2 \rightarrow \sum_{n=0}^{\infty} \omega_n$, and the ω_n is the degeneracy of the n -th electron Landau level in relativistic magnetic field, and can be calculated by (Canuto et al. 1971; Kubo. 1965; Pathria 2003)

$$\omega_n = \frac{1}{h^2} \int_0^{2\pi} d\phi \int_{k_1 < p_{\perp}^2 < k_2} p_{\perp} dp_{\perp} = \frac{2\pi (k_2 - k_1)}{h^2 \cdot 2}$$

$$= \frac{1}{2\pi} \left(\frac{\hbar}{m_e c} \right)^{-2} \frac{B}{B_{\text{cr}}} = \frac{b}{2\pi} \left(\frac{\hbar}{m_e c} \right)^{-2}, \quad (50)$$

where $k_1 = 2nm_e^2 c^2 \frac{B}{B_{\text{cr}}} = 2nbm_e^2 c^2$, and $k_2 = 2(n+1)bm_e^2 c^2$.

Based on the works of Peng et al. (2007); Gao et al. (2013), which introduced the Dirac δ -function and considered Pauli exclusion principle, we discuss the SES problem in a SMF. Our results show that the stronger the magnetic field, the higher Fermi energy of electrons becomes. The ESP increases with SMF and the maximum value of ESP is 0.1 MeV in a SMF. The SEF also increases greatly and its maximum approaches to 5.0 MeV (e.g. $\rho_7 = 0.01, T_9 = 0.2, B_{12} = 10^3 \text{G}$).

4.2. Investigation of the nuclear reaction rates

In the explosive hydrogen burning stellar environments, the nuclear reaction $^{23}\text{Mg}(p, \gamma)^{24}\text{Al}$ plays a key role because of breaking out the Ne-Na cycle to heavy nuclear species (i.e., Mg-Al cycle). Therefore, it is very important to accurately determine the rates for the reaction $^{23}\text{Mg}(p, \gamma)^{24}\text{Al}$. However, the resonance energy has a large uncertainty due to the inconsistent $^{24}\text{Mg}(^3\text{He}, t)^{24}\text{Al}$ measurements mentioned. So it may lead to a factor of 5 variation in the reaction rate at $T_9 = 0.25$ because of its exponential dependence on E_r (Visser et al. 2007). Some authors discussed the contributions from several important resonance states, such as (Wallace et al. 1981; Wiescher et al. 1986; Kubono et al. 1995; Visser et al. 2007). In order to reduce the uncertainty of the reaction rates in this paper, we reference some information about this reaction and the values of the E_r, E_x and corresponding to $\omega\gamma_i$ and some average values of $\omega\gamma_i$ are adopted and listed in Table 2. According to these information, we analyze the total rates for these five SES models.

Tables 3 and 4 give a brief description of the factor S_i ($i = 1, 2, 3$) for LD, FGP, and LJ models when $B_{12} = 10, 10^3$, respectively. As the density and temperature increase, the

Table 1: The comparisons of the resonant SEFs for Dewitt, Liolios, LD, FGP and LJ models in several typical astronomical conditions. The former two models are in the case without SES and SMFs, while the latter three models are in the case with SES and SMFs.

		$B_{12} = 10$					$B_{12} = 10^3$		
ρ_7	T_9	$F_r^0(\text{Lios})$	$F_r^0(\text{Dew})$	$F_r^B(\text{LD})$	$F_r^B(\text{FGP})$	$F_r^B(\text{LJ})$	$F_r^B(\text{LD})$	$F_r^B(\text{FGP})$	$F_r^B(\text{LJ})$
0.01	0.1	1.7475	3.8973	1.6956	1.6964	0.1749	1.0725e-15	1.3472e-13	25.5680
0.05	0.1	1.7475	10.9451	1.6956	1.7013	8.4513e-4	1.0725e-15	0.6045	19.5717
0.1	0.2	1.3219	4.3605	1.3021	1.3045	0.0022	3.2750e-8	2.4894	3.8848
0.1	0.3	1.2051	2.5873	1.1922	1.1941	0.0174	1.0221e-5	1.8371	2.4713
0.2	0.3	1.2045	3.3934	1.1924	1.1939	9.1604e-4	1.0236e-5	2.4990	2.1361
0.3	0.4	1.1497	2.8170	1.1411	1.1422	7.7822e-4	1.8097e-4	2.1178	1.6055
1.0	0.5	1.1181	3.5124	1.1113	1.1122	6.2630e-7	0.0011	1.9290	0.9512
10	0.7	1.0830	7.2692	1.0780	1.0791	6.2012e-9	0.0072	1.6142	0.0894

results of LD model are in good agreement with those of FGP, but disagreement with our results at $B_{12} = 10$. This is because that the electron Fermi energy of our model is lower than those of LD and FGP in relatively low magnetic fields. As the magnetic fields increase from $B_{12} = 10$ to 10^3 , the factor S_3 increases about 2 ~ 3 orders magnitude (i.e., from 0.1749 to 25.5680 and from 0.0022 to 3.8848) when $\rho_7 = 0.01, T_9 = 0.1$ and $\rho_7 = 0.1, T_9 = 0.2$, respectively. When $B_{12} = 10^3$ the factor S_3 is about 39.74, 5.69, 1.56 times larger than S_2 (FGP model) at $\rho_7 = 0.03, T_9 = 0.2$, $\rho_7 = 0.05, T_9 = 0.2$ and $\rho_7 = 0.1, T_9 = 0.2$, respectively. From what has been discussed above, the LD model maybe only adapts to the relatively low magnetic field and low density surroundings. The FGP and LD models are both unadapted to relatively low density, and high magnetic field surroundings (e.g. $\rho_7 < 0.1, B_{12} > 10^2$). However, our model can be well adapted to relatively high magnetic field and low density surroundings (e.g. $B_{12} > 10^2, \rho_7 < 0.05$).

Table 2: Resonance parameters for the reaction $^{23}\text{Mg} (p, \gamma) ^{24}\text{Al}$.

E_x (MeV) ^a	E_x (MeV) ^b	J^π	E_{r_i} (MeV) ^c	Γ_p	Γ_γ	$\omega\gamma_i$ (meV) ^d	$\omega\gamma_i$ (meV) ^e	$\omega\gamma_i$ (meV) ^f
2.349±0.020	2.346±0.000	3 ⁺	0.478	185	33	25	27	26
2.534±0.013	2.524±0.002	4 ⁺	0.663	2.5e3	53	58	130	94
2.810±0.020	2.792±0.004	2 ⁺	0.939	9.5e5	83	52	11	31.5
2.900±0.020	2.874±0.002	3 ⁺	1.029	3.4e4	14	12	16	14

^ais adopted from Ref. (Endt 1998)

^bfrom Ref.(Visser et al. 2007)

^c from Ref.(Audi et al. 1995)

^d from Ref.(Herndl et al. 1998)

^efrom Ref.(Wiescher et al. 1986)

^fis adopted in this paper

Summing up the above discussions, our calculations show that this SES effect in a SMF can increase nuclear reaction rates of $^{23}\text{Mg} (p, \gamma)^{24}\text{Al}$ by several orders magnitude. A more precise thermonuclear rates of $^{23}\text{Mg} (p, \gamma)^{24}\text{Al}$ will help us to constrain the determination of nuclear flow out of the Ne-Na cycle, and production of $A \geq 20$ nuclides, in explosive hydrogen burning over a temperature range of $0.2 \leq T \leq 1.0$ GK.

5. Conclusions

In this paper, based on the relativistic theory in a SMF, we investigate the problem of SES, and the SES influence on the nuclear reaction of $^{23}\text{Mg} (p, \gamma)^{24}\text{Al}$ by LD, FGP, and LJ strong screening models in a SMF. The results show that the SES thermonuclear reaction rates have a remarkable increase in a SMF. The rates can increase by around three orders of magnitude. For example, when B_{12} increases from 10 to 10^3 , the rates increase from 0.1749 to 25.5680 at $\rho_7 = 0.01, T_9 = 0.1$, and from 0.0022 to 3.8848 at $\rho_7 = 0.1, T_9 = 0.2$. The

Table 3: Comparisons of the rates of λ_r^0 , which are in the case without SES with those of the LD ($\lambda_r^{\text{scB}}(\text{LD})$), FGP ($\lambda_r^{\text{scB}}(\text{FGP})$) and our calculations $\lambda_r^{\text{scB}}(\text{LJ})$ in the case with SES for some typical astronomical conditions at $B_{12} = 10$, respectively. $S_i = \lambda_{ri}^{\text{scB}}/\lambda_r^0$, $i = 1, 2, 3$ denote the rates of LD, FGP, and LJ model, respectively.

ρ_7	T_9	λ_r^0	$B_{12} = 10$			S_1	S_2	S_3
			$\lambda_r^{\text{scB}}(\text{LD})$	$\lambda_r^{\text{scB}}(\text{FGP})$	$\lambda_r^{\text{scB}}(\text{LJ})$			
0.01	0.1	1.0942e-19	1.8552e-19	1.8561e-19	1.9138e-20	1.6956	1.6964	0.1749
0.02	0.1	1.0942e-19	1.8552e-19	1.8598e-19	4.0569e-21	1.6956	1.6998	0.0371
0.03	0.1	1.0942e-19	1.8552e-19	1.8608e-19	1.0413e-21	1.6956	1.7007	0.0095
0.03	0.2	4.2967e-8	5.5949e-8	5.6034e-8	4.1916e-9	1.3021	1.3041	0.0976
0.04	0.2	4.2967e-8	5.5949e-8	5.6041e-8	2.2448e-9	1.3021	1.3043	0.0522
0.05	0.2	4.2967e-8	5.5949e-8	5.6044e-8	1.2491e-9	1.3021	1.3043	0.0291
0.1	0.2	4.2967e-8	5.5949e-8	5.6051e-8	9.3383e-11	1.3021	1.3045	0.0022
0.2	0.4	0.0163	0.0186	0.0186	8.5713e-5	1.1411	1.1422	0.0053
0.3	0.5	0.1925	0.2140	0.2141	6.2713e-4	1.1114	1.1122	0.0033
0.5	0.6	0.9764	1.0663	1.0669	8.5404e-4	1.0920	1.0927	8.7465e-4
0.7	0.8	7.2550	7.7500	7.7537	0.0079	1.0682	1.0687	0.0011
1.0	0.9	14.0604	14.9100	14.9162	0.0050	1.0604	1.0609	3.5785e-4

considerable increase in the reaction rates for $^{23}\text{Mg} (p, \gamma) ^{24}\text{Al}$ implies that more ^{23}Mg will escape the Ne-Na cycle due to SES in a SMF. Then it will make the next reaction convert more $^{24}\text{Al} (\beta^+, \nu) ^{24}\text{Mg}$ to participate in the Mg-Al cycle. It may lead to synthesizing a large amount of heavy elements at the crust of magnetars. These heavy elements, which are produced from the nucleosynthesis process, may be thrown out due to the compact binary mergers of double neutron star (NS-NS) or black hole and neutron star (BH and NS) systems. On the other hand, our model for the rates is in good agreement with those of LD and FGP models at relatively low density (e.g., $\rho_7 < 0.01$) and $B_{12} < 10^2$. In relatively low magnetic fields (e.g., $B_{12} < 1$), the SES of LD and FGP models have strong influence on the rates compare to our model. However, the rates in our model can be about 1.58 times

Table 4: Comparisons of the rates of λ_r^0 , which are in the case without SES and SMFs with those of the LD ($\lambda_r^{\text{scB}}(\text{LD})$), FGP ($\lambda_r^{\text{scB}}(\text{FGP})$) and our calculations $\lambda_r^{\text{scB}}(\text{LJ})$ in the case with SES for some typical astronomical conditions at $B_{12} = 10^3$, respectively. The S_i is the same as in Table 3.

ρ_7	T_9	λ_r^0	$B_{12} = 10^3$			S_1	S_2	S_3
			$\lambda_r^{\text{scB}}(\text{LD})$	$\lambda_r^{\text{scB}}(\text{FGP})$	$\lambda_r^{\text{scB}}(\text{LJ})$			
0.01	0.1	1.0942e-19	1.1735e-34	1.4740e-32	2.7975e-18	1.0725e-15	1.3472e-13	25.5680
0.02	0.1	1.0942e-19	1.1735e-34	6.4612e-24	2.5883e-18	1.0725e-15	5.9052e-5	23.6555
0.03	0.1	1.0942e-19	1.1735e-34	1.5306e-21	2.4177e-18	1.0725e-15	0.0140	22.0969
0.03	0.2	4.2967e-8	1.4072e-15	5.0819e-9	2.0198e-7	3.2750e-8	0.1183	4.7007
0.04	0.2	4.2967e-8	1.4072e-15	1.7120e-8	1.9575e-7	3.2750e-8	0.3984	4.5559
0.05	0.2	4.2967e-8	1.4072e-15	3.3408e-8	1.9009e-7	3.2750e-8	0.7775	4.4240
0.1	0.2	4.2967e-8	1.4072e-15	1.0696e-7	1.6692e-7	3.2750e-8	2.4894	3.8848
0.2	0.4	0.0163	2.9459e-6	0.0324	0.0288	1.8097e-4	1.9876	1.7669
0.3	0.5	0.1925	1.9523e-4	0.3509	0.2812	0.0010	1.8227	1.4604
0.5	0.6	0.9764	0.0031	1.6579	1.1949	0.0032	1.6979	1.2237
0.7	0.8	7.2550	0.0976	10.8789	7.8159	0.0135	1.4995	1.0773
1.0	0.9	14.0604	0.3053	20.2526	13.6742	0.0217	1.4404	0.9725

and three orders magnitude higher than those of FGP and LD in relatively high magnetic fields and low density surroundings (e.g., $B_{12} \geq 10^2$, $\rho_7 < 0.05$), respectively. The results we derived, may have very important implications in some astrophysical applications for the nuclear reaction, the thermal evolution, and numerical simulation of magnetars.

We would like to thank the anonymous referee for carefully reading the manuscript and providing some constructive suggestions which are very helpful to improve this manuscript. This work was supported in part by the National Natural Science Foundation of China under grants 11565020, and the Counterpart Foundation of Sanya under grant 2016PT43, the Special Foundation of Science and Technology Cooperation for Advanced Academy and

Regional of Sanya under grant 2016YD28, the Scientific Research Starting Foundation for 515 Talented Project of Hainan Tropical Ocean University under grant RHDRC201701, and the Natural Science Foundation of Hainan Province under grant 114012.

REFERENCES

- R. K. Wallace, & S. E. Woosley, *ApJS.*, **45**: 389 (1981).
- C. Iliadis, J. M. D’Auria, S. Starrfield, et al., *ApJS*, **134**: 151 (2001)
- S. Kubono, T. Kajino, & S. Kato, *Nucl. Phys. A.*, **588**: 521(1995)
- H. Herndl, , M. Fantini, C. Iliadis, P. M. Endt, & H. Oberhummer, *Phys. Rev. C.*, **58**: 1798 (1998)
- D. W. Visser, , Wrede, C., J. A. Caggiano, et al., *Phys. Rev. C.*, **76**: 5803 (2007)
- G. Lotay, P. J. Wood, D. Seweryniak, et al., *Phys. Rev. C.*, **77**: 2802 (2008)
- J. N. Bahcall, L. Brown, A. Gruzinov, & R. Sawyer, *A&A* **383**: 291 (2002)
- J. J. Liu, *MNRAS*, **433**: 1108 (2013)
- J. J. Liu, *MNRAS*, **438**: 930 (2014)
- J. J. Liu, *RAA*, **16**: 83 (2016)
- J. J. Liu, W. M. Gu., *ApJS*, **224**: 29 (2016)
- J. J. Liu, et al., *RAA*, **17**: 107 (2017)
- J. J. Liu, et al., *ChPhC*, **41**:095101 (2017)
- E. E. Salpeter, & H. M. van Horn, *ApJ*, **155**: 183 (1969)
- E. E. Salpeter, *AuJPh.*, **7**: 373 (1954)
- H. C. Graboske, & H. E. DeWitt, *ApJ*, **181**: 457 (1973)
- H. E. Dewitt, *Phys. Rev. A.*, **14**: 1290 (1976)

- T. E. Liolios, EPJA., **9**: 287 (2000)
- T. E. Liolios, Phys. Rev. C., **64**: 8801 (2001)
- P. A. Kravchuk, & D. G. Yakovlev, Phys. Rev. C., **89**: 5802 (2014)
- Q. H. Peng, & H. Tong, MNRAS, **378**: 159 (2007)
- Z. F. Gao., N. Wang, J. P. Yuan, L. Jiang, D. L. Song, Ap&SS, **332**: 129(2011)
- Z. F. Gao, N. Wang, Q. H. Peng, X. D. Li, & Y. J. Du, Mod. Phys. Lett. A., **28**: 50138 (2013)
- Z. F. Gao., N. Wang, Y. Xu, H. Shan, X. D. Li., AN, **336**: 866(2015)
- Z. F. Gao., N. Wang, H. Shan, X. D. Li, W. Wang, ApJ, eprint arXiv:1709.03459
- Z. F. Gao., Y. Xu, H. Shan, X. D. Li., H. Shan, W. Wang, N. Wang., AN, eprint arXiv:1709.02186 (2017)
- X. H. Li, Z. F. Gao, X. D. li, et al., IJMPD, **25**: 1650002(2016)
- D. Lai, & S. L. Shapiro, ApJ, **383**: 745 (1991)
- D. Lai, Rev. Mod. Phys., **73**: 629 (2001)
- R. C. Duncan, & C. Thompson, ApJ, 392, 9 (1992)
- I. Fushiki, E. H. Gudmundsson, & C. J. Pethick, ApJ, **342**: 958 (1989)
- L. D. Landau, & E. M. Lifshitz, *Quantum mechanics*, (3rd ed., Oxford: Pergamon Press 1977), p.457
- C. Zhu, Z. F. Gao., X. D. Li.et al., Mod. Phys. Lett. A., **31**: 50070(2016)

- N. W. Ashcroft, & N. D. Mermin, *Solid State Physics*, (Saunders College: Philadelphia 1976), p.123
- B. B. Kadomtsev, O. P. Pogutse, *Phys. Rev. L.* **25**: 1155 (1971)
- J. M. Lattimer, C. J. Pethick, D. G. Ravenhall, & D. Q. Lamb, *Nucl. Phys. A.*, **432**: 646 (1985)
- W. Stolzmann, & T. Bloecker, *A&A*, **314**: 1024 (1996)
- D. G. Yakovlev, & D. A. Shalybkov, *Astrophys. Space. Phys. Rev.*, **7**: 311 (1989)
- W. A. Fowler, G. R. Caughlan, & B. A. Zimmerman, *ARA&A.*, **5**: 525 (1967)
- A. M. Lane, & R. G. Thomas, *Rev. Mod. Phys.*, **30**: 257 (1958)
- H. Schatz, A. Aprahamian, J. Goerres, et al., *Phys. Rep.*, **294**: 167 (1998)
- Canuto, V., & H. Y. Chiu, *Phys. Rev.*, **173**: 1210 (1968)
- Canuto, V., & H. Y. Chiu, *Space. Sci. Rev.*, **12**: 3 (1971)
- R. Kubo, *Statistics Mechanics*, (Amsterdam: North-Holland Publishing Co.1965) p.278
- R. K. Pathria, *Statistics Mechanics*, (2nd. Singapore: Isevier 2003), p.280
- M. Wiescher, J. Gorres, F.-K. Thielemann, & H. Ritter, *A&A*, **160**: 56 (1986)
- P. M. Endt, *Nucl. Phys. A.*, **633**: 1 (1998)
- G. Audi, & A. H. Wapstra, *Nucl. Phys. A.*, **595**: 409 (1995)

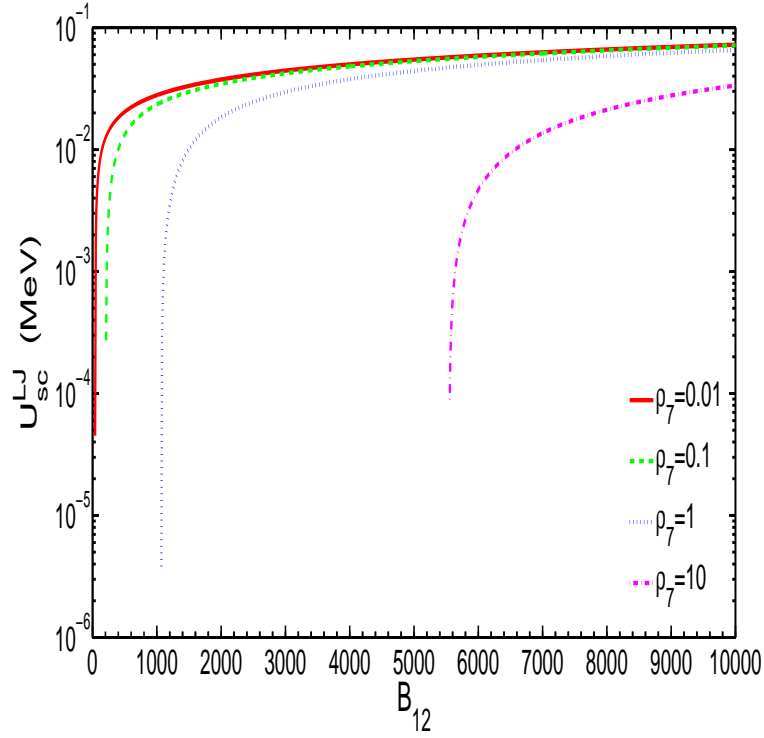


Fig. 1.— The electron screening potential as a function of B_{12} of LJ model for some typical astronomical condition.

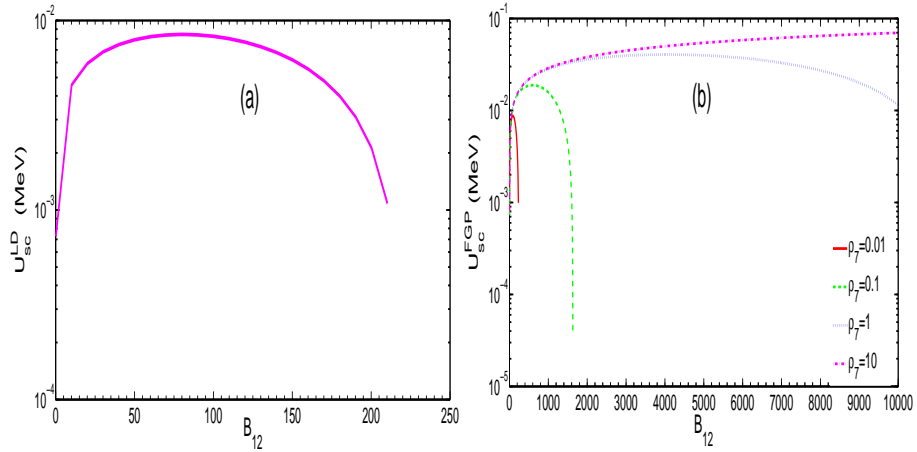


Fig. 2.— The electron screening potential as a function of B_{12} in LD, and FGP models for some typical astronomical condition.

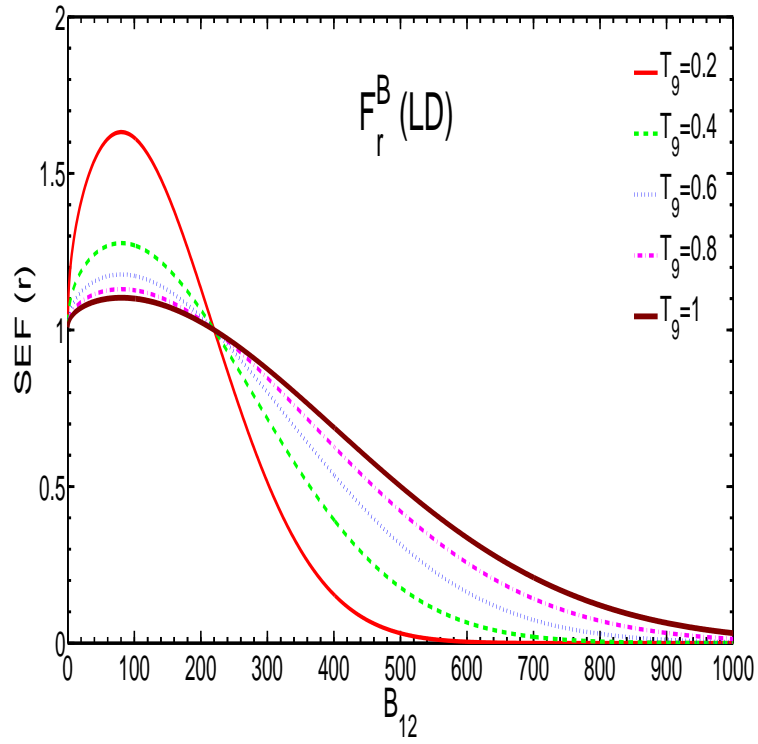


Fig. 3.— The resonant SEF for LD model as a function of B_{12} in the case with SES and SMF.

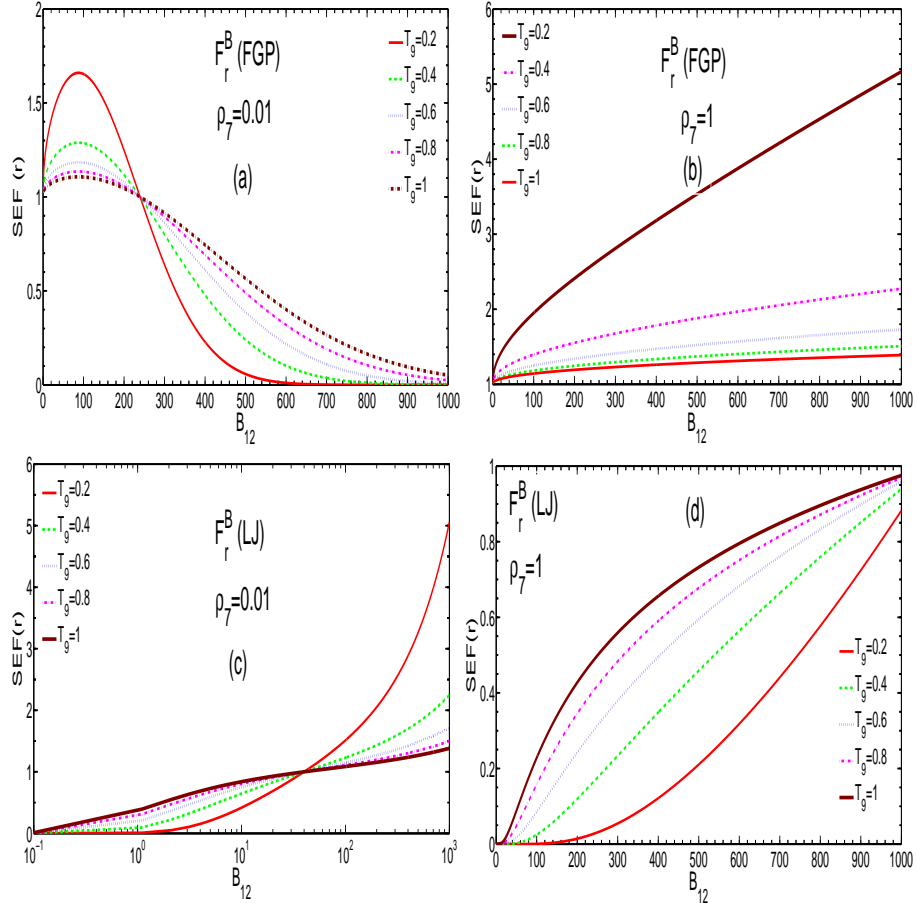


Fig. 4.— The resonant SEF for FGP and LJ models as a function of B_{12} in the case with SES and SMF.

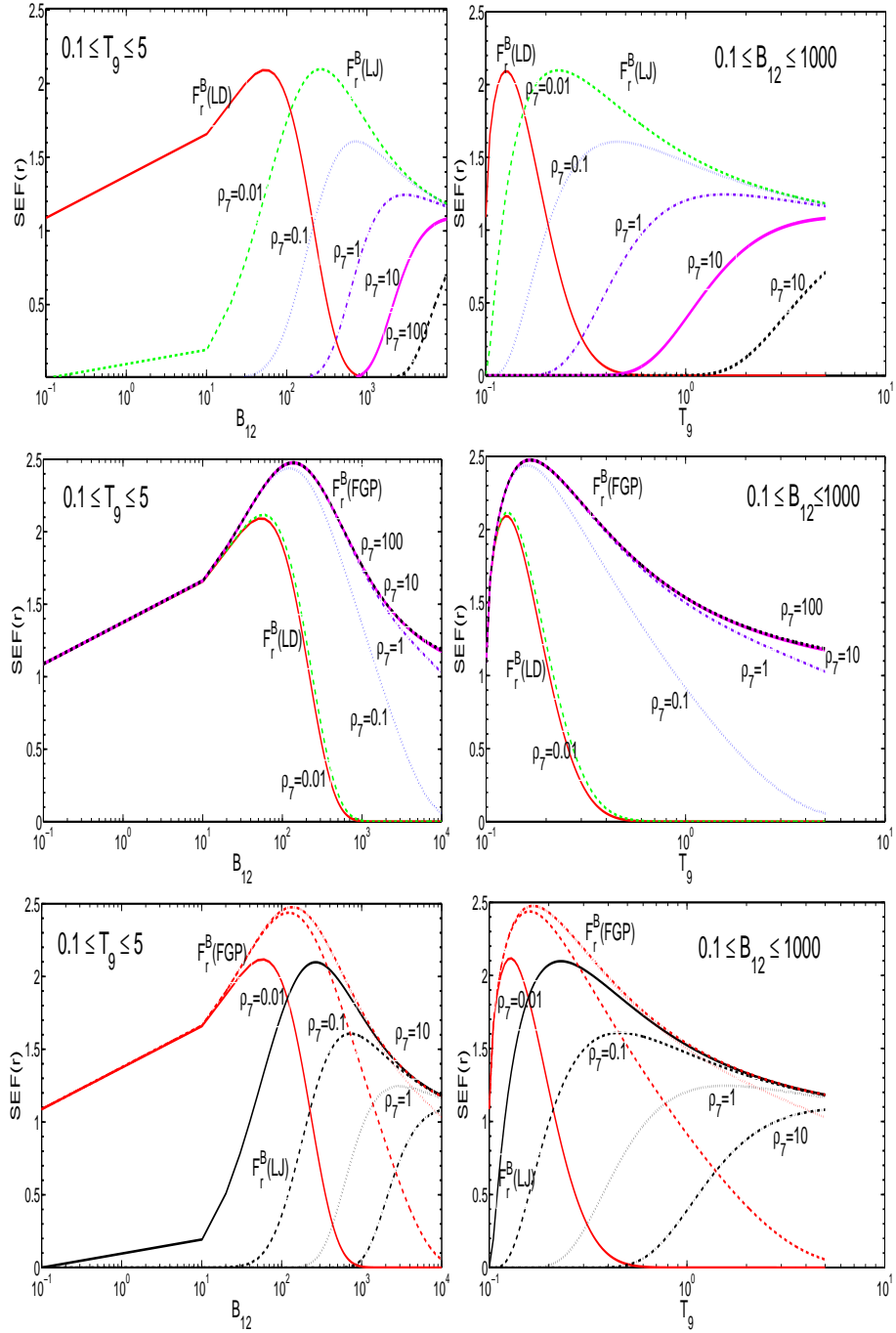


Fig. 5.— The comparisons are plotted for some typical astronomical condition of the resonant SEF among the three models of LJ, LD, and FGP in the case with SES and SMF.

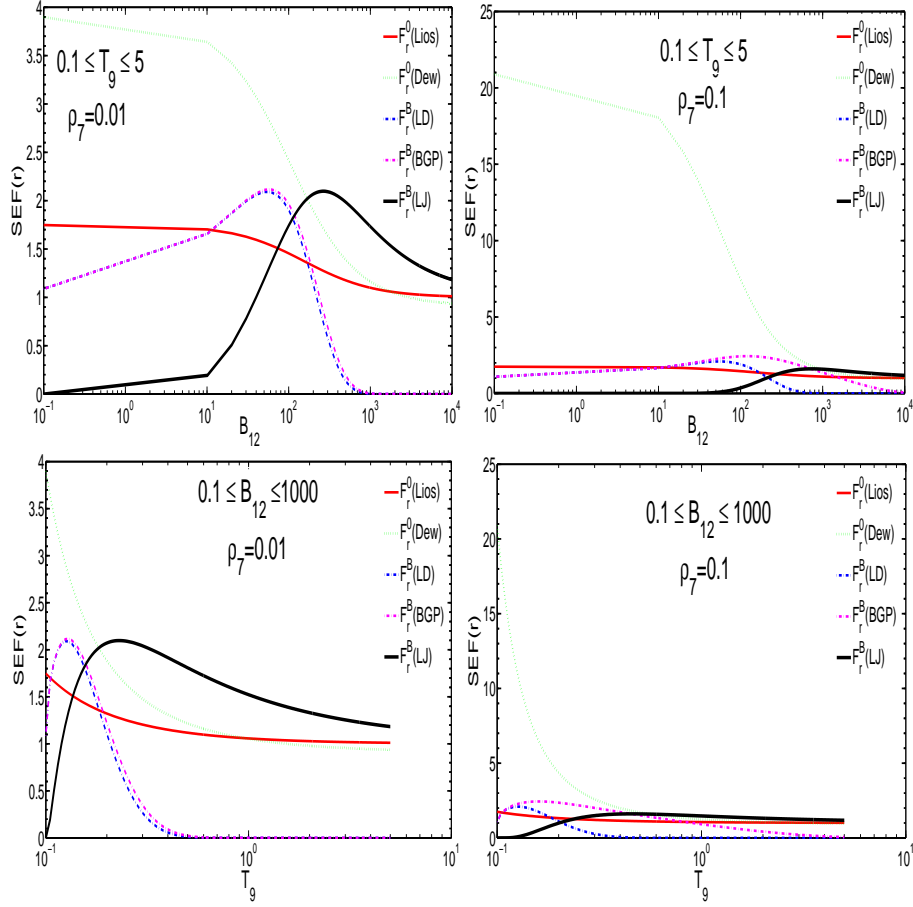


Fig. 6.— The comparisons of the resonant SEF for the model of Liolios, Dewitt with those of models of LD, FGP, and LJ.